Supporting Information

Development of photoluminescent hydrogen bonded frameworks based on pyromellitic diimide tethered carboxylic acid hosts and multi-bonding solvent guests

Raju Ram Puniya‡[a], Priyanka Takhar‡[a], Monika Chhapoliya, Rinki Deka[b], Dhruba Jyoti Kalita[b], Devendra Singh*[a]

[a]Department of Chemistry, Mohanlal Sukhadia University, Udaipur-313001, Rajasthan, INDIA.

[b]Department of Chemistry, Gauhati University, Guwahati-781014, Assam, INDIA.

Email: dsingh@mlsu.ac.in

List of Contents

Experimental

Materials and methods

All reagents and solvents were purchased from commercial sources. FT-IR spectra were recorded on a PerkinElmer-Spectrum One FT-IR spectrometer with KBr disks in the range 4000−400 cm^{-1}. The UV−Vis and fluorescence emission spectra were recorded on a Perkin-Elmer-Lambda750 UV−vis spectrometer and Perkin-Elmer-LS55 fluorescence spectrometer, respectively, at room temperature. Thermogravimetric analyses and differential scanning calorimetry experiments were performed on Mettler Toledo Q500 TA and Q200 TA instruments, respectively. In both cases, samples were placed in open alumina pans in the temperature range 25−500 °C and were purged with a stream of dry N_2 flowing at 100 mL min^{-1}. ^1H NMR and ^{13}C NMR spectra were recorded using a 400 MHz FT-NMR Bruker Advance III HD instrument. Chemical shifts were reported in parts per million (ppm) relative to internal TMS (0 ppm). Electrospray ionization mass (ESI-MS) spectra were recorded on a Waters (Micromass MS Technologies) Q-Tof Premier mass spectrometer. PXRD data were collected on a Bruker D8 Advance diffractometer in Bragg−Brentano $\theta-\theta$ geometry with CuKα radiation on a glass surface of an air-dried sample using a secondary curved graphite monochromator. Diffraction patterns were collected over a 2θ range of 5−50° at a scan rate of 2° min^{-1}.

Computational Details

Hydrogen bond motifs are derived from formic acid and its interaction with DMF and pyridine solvent molecules as a model system. All the calculations are performed using the Gaussian09 program package in the gas phase.[S1] The energies of the geometries of these models are calculated by DFT[S2] using Becke's three-parameter exchange functional[S3] along with the gradient-corrected functional of Lee, Yang and Parr (B3LYP and B3LYP-D3 functionals).[S4] Single point calculations at the 6-31+G*, 6-31++G*, 6-31++G** and AUG-cc-pVDZ levels are performed on the fully optimized geometries of levels B3LYP/6-31+G* and B3LYP-D3/6-31+G*, respectively. The interaction energy (E_{int}) for each multi-molecular motif was obtained by $E_{int} = [E_{\text{for multimolecular structure}} - (E_{\text{for formic acid}} + E_{\text{for interacting solvent molecules}})]$. The relative stability of a particular motif over another motif was calculated by subtracting the value of lower energy motif from the higher energy motif.

Crystal Structure Determination

Crystals are coated with Paratone oil, and the diffraction data are collected at 173 K with MoKα radiation on a Rigaku Rapid Auto Diffractometer equipped with a graphite crystal incident beam monochromator. The Rapid Auto software [S5] is used for data collection and data processing. The structures are solved by direct method and refined by full-matrix least-squares calculation with the SHELXTL software package.[S6] All non-hydrogen atoms are refined anisotropically; the hydrogen atoms are assigned isotropic displacement coefficients U(H) = 1.2U (C) and 1.5U (C_{methyl}), and their coordinates are allowed to ride on their respective atoms. In the structures of solvates **2b** and **2d**, all three carbon atoms in the aliphatic part attached with cyclic imide cores are found to be disordered. These disordered atoms are refined by sharing two carbon atoms at one position having half occupancies and then hydrogen atoms are fixed at respective positions. Both the oxygen atoms of carboxylic acid groups are also disordered and treated in a similar manner in case of structure **2d**. The disordered nitrogen atom of guest quinoline is also refined by sharing carbon and nitrogen atoms at one position with half occupancies in this structure. The crystallographic details and hydrogen bond parameters are listed in Table S4 and Table S5, respectively. The CCDC 2324804-2324810 contains the supplementary crystallographic data for this paper.

Synthesis and characterization of host compounds 1, 2 and their solvates

Compound **1**: A solution of pyromellitic dianhydride (1.090 gm, 5 mmol) and 3-aminobutanoic acid (1.0312 gm, 10 mmol) in acetic acid (50 mL) was refluxed for 3 hrs. This solution was cooled to room temperature, poured into ice cooled water (100 mL) and stirred for 30 min. A white colored precipitate of the product was obtained. This precipitate of the product was filtered, washed several times with water and air-dried. Yield: 86%. IR (KBr, cm^{-1}): 3432 (bm), 1769 (s), 1715 (s), 1637 (w), 1392 (m), 1354 (s), 1230 (s), 1140 (m), 1081(m), 1024 (s), 829 (s), 732 (s), 569 (w). ^{1}H NMR (400 MHz, DMSO-d_6): 12.33 (s, 2H), 8.17 (s, 2H), 4.62 (dd, 2H, J = 4.8 Hz), 2.98 (dd, 2H, J = 5.6 Hz), 2.79 (dd, 2H, J = 4.4 Hz), 1.41 (d, 6H, J = 4.8 Hz). ^{13}C NMR (DMSO-d_6): 171.99, 166.02, 136.80, 117.28, 43.77, 37.69, 18.26 ESI-MS: 389.33 ($M + H^+$).

Solvate **1a**: Compound **1** was dissolved in DMF and left undisturbed for few days. Colourless block crystals of **1a** were obtained in good yield. IR (KBr, cm^{-1}): 3465 (bm), 2936 (w), 2362 (m), 1768 (s), 1715 (s), 1648 (m), 1435 (m), 1392 (m), 1355 (s), 1307 (m), 1226 (s), 1156 (m),

1108 (s), 1081 (s), 1025 (s), 915 (m), 828 (s), 732 (s), 671 (s), 595 (m), 567 (m) ^{1}H NMR (400 MHz, DMSO-d_6): 12.32 (s, 2H), 8.17 (s, 2H), 7.94 (s, 2H), 4.63 (dd, 2H, *J* = 4.8 Hz), 2.98 (dd, 2H, *J* = 5.2 Hz), 2.89 (s, 6H), 2.79 (dd, 2H, *J* = 4.8 Hz), 2.73 (s, 6H), 1.41 (d, 6H, *J* = 4.8 Hz).

Solvate **1b**: Colorless needle shaped crystals of **1b** were obtained from the solution of compound **1** in pyridine solvent. IR (KBr, cm^{-1}): 3433 (bm), 2992 (m), 2449 (w), 1763 (m), 1709 (s), 1598 (m), 1438 (m), 1380 (m), 1352 (s), 1319 (s), 1247 (m), 1215 (m), 1149 (m), 1112 (m), 1065 (m), 1027 (s), 1008 (m), 914 (m), 868 (m), 824 (s), 753 (m), 731 (s), 703 (s), 631 (m), 595 (m), 563 (m) ^{1}H NMR (400 MHz, DMSO-d_6): 12.33 (s, 2H), 8.57 (d, 4H, *J* = 2.8 Hz), 8.17 (s, 2H), 7.78 (m, 2H), 7.38 (m, 4H), 4.63 (dd, 2H, *J* = 4.4 Hz), 2.99 (dd, 2H, *J* = 5.2 Hz), 2.79 (dd, 2H, *J* = 4.8 Hz), 1.41 (d, 6H, *J* = 4.8 Hz).

Solvate **1c**: Solvate **1c** was crystallized from the solution of **1** in quinoline solvent. IR (KBr, cm^{-1}): 3466 (bm), 2997 (m), 2454 (w), 1931 (w), 1765 (s), 1715 (s), 1595 (m), 1505 (s), 1457 (m), 1427 (m), 1378 (m), 1354 (s), 1312 (s), 1246 (m), 1214 (s), 1152 (s), 1124 (m), 1078 (m), 1026 (s), 952 (m), 913 (s), 868 (m), 814 (s), 784 (s), 768 (m), 730 (s), 627 (m), 597 (m), 563 (m), 527 (m), 481 (s) ^{1}H NMR (400 MHz, DMSO-d_6): 12.34 (s, 2H), 8.90 (d, 2H, *J* = 1.2 Hz), 8.36 (d, 2H, *J* = 5.2 Hz), 8.15 (s, 2H), 7.99 (dd, 4H, *J* = 5.6 Hz), 7.76 (m, 2H), 7.61 (t, 2H, *J* = 4.4 Hz), 7.53 (dd, 2H, *J* = 2.8 Hz), 4.64 (dd, 2H, *J* = 4.4 Hz), 2.99 (dd, 2H, *J* = 5.2 Hz), 2.79 (dd, 2H, *J* = 4.8 Hz), 1.41 (d, 6H, *J* = 4.4 Hz).

Compound **2**: A solution of pyromellitic dianhydride (1.090 gm, 5 mmol) and 3-amino-2-methylpropanoic acid (1.0312 gm, 10 mmol) in acetic acid (40 mL) was refluxed for 3 hrs. The reaction mixture was cooled to room temperature, poured into ice cooled water (80 mL) and stirred for 30 min. A white color precipitate of the product was filtered, washed several times with water and air-dried. Yield: 92%. IR (KBr, cm^{-1}): 3464 (bm), 3034 (m), 2361 (m), 1171 (m), 1710 (s), 1465 (m), 1400 (s), 1364 (m), 1337 (m), 1311 (m), 1238 (s), 1165 (m), 1131 (m), 1074 (m), 1041 (s), 952 (m), 900 (m), 831 (m), 804 (m), 728 (s), 601 (s), 560 (m), 531 (m) ^{1}H NMR (400 MHz, DMSO-d_6): 12.46 (s, 2H), 8.23 (s, 2H), 3.85 (dd, 2H, *J* = 4.8 Hz), 3.63 (dd, 2H, *J* = 5.2 Hz), 2.82 (dd, 2H, *J* = 4.8 Hz), 1.08 (d, 6H, *J* = 4.4 Hz) ^{13}C NMR (DMSO-d_6): 174.78, 166.04, 136.782, 117.30, 40.60, 37.65, 14.57 ESI-MS: 389.32 (M + H$^+$).

Solvate **2a**: Solvate **2a** was crystallized from the DMF solution of compound **2** as colorless block crystals. IR (KBr, cm^{-1}): 3465 (bm), 2942 (bm), 1944 (w), 1771 (m), 1710 (s), 1630 (m), 1465

(m), 1430 (m), 1400 (s), 1379 (m), 1330 (m), 1220 (m), 1168 (m), 1105 (s), 1071 (s), 1042 (s), 952 (m), 897 (m), 834 (m), 804 (m), 729 (s), 670 (s), 599 (s), 560 (s) ^{1}H NMR (400 MHz, DMSO-d_6): 12.45 (s, 1H), 8.23 (s, 2H), 7.95 (s, 2H), 3.86 (dd, 2H, J = 4.8 Hz), 3.65 (dd, 2H, J = 5.2 Hz), 2.89 (s, 6H), 2.82 (dd, 2H, J = 4.8 Hz), 2.73 (s, 6H), 1.09 (d, 6H, J = 4.8 Hz).

Solvate **2b**: Crystals of **2b** were obtained by crystallization of **2** in pyridine as colorless needles. IR (KBr, cm^{-1}): 3433 (bm), 3035 (m), 2361 (m), 1771 (m), 1709 (s), 1463 (m), 1399 (s), 1365 (m), 1237 (m), 1169 (m), 1129 (m), 1073 (m), 1042 (s), 910 (m), 832 (m), 804 (m), 728 (s), 706 (m), 600 (m), 560 (m) ^{1}H NMR (400 MHz, DMSO-d_6): 12.45 (s, 2H), 8.57 (d, 4H, J = 2.8), 8.23 (s, 2H), 7.78 (m, 2H), 7.38 (dd, 4H, J = 3.6 Hz), 3.86 (dd, 2H, J = 4.8 Hz), 3.65 (dd, 2H, J = 5.2 Hz), 2.82 (dd, 2H, J = 4.8 Hz), 1.09 (d, 6H, J = 4.4 Hz).

Solvate **2c**: A solution of compound **2** in quinoline solvent was resulted in the formation of brown colored block shaped crystals of **2c**. IR (KBr, cm^{-1}): 3437 (bm), 1770 (m), 1505 (m), 1459 (m), 1395 (s), 1348 (s), 1316 (m), 1213 (s), 1156 (m), 1121 (m), 1038 (s), 951 (m), 894 (m), 812 (s), 785 (s), 767 (m), 728 (s), 626 (m), 597 (m), 559 (m), 480 (s) ^{1}H NMR (400 MHz, DMSO-d_6): 12.47 (s, 2H), 8.90 (d, 2H, J = 2.8 Hz), 8.36 (d, 2H, J = 5.6 Hz), 8.21 (s, 2H), 7.99 (dd, 4H, J = 5.6 Hz), 7.76 (t, 2H, J = 4.8 Hz), 7.61 (t, 2H, J = 4.8 Hz), 7.53 (dd, 2H, J = 2.8 Hz), 3.86 (dd, 2H, J = 4.8 Hz), 3.65 (dd, 2H, J = 5.2 Hz), 2.82 (dd, 2H, J = 5.2 Hz), 1.09 (d, 6H, J = 4.8 Hz).

Solvate **2d**: A solution of compound **2** in piperidine solvent in the presence of small amount of quinoline solvent (1-2 drops) was resulted in the formation of crystals of mixed solvate **2d**. IR (KBr, cm^{-1}): 3466 (bm), 2978 (s), 2361 (m), 1766 (m), 1715 (s), 1505 (m), 1457 (m), 1378 (w), 1354 (s), 1312 (m), 1214 (m), 1152 (m), 1125 (w), 1026 (s), 953 (w), 914 (m), 814 (m), 785 (s), 784 (w), 730 (m), 628 (w), 597 (m), 564 (m), 481 (m) ^{1}H NMR (400 MHz, DMSO-d_6): 12.34 (s, 2H), 8.87 (d, 1H, J = 3.6 Hz), 8.34 (d, 1H, J = 5.6 Hz), 8.13 (s, 2H), 7.96 (dd, 2H, J = 5.6 Hz), 7.75 (t, 1H, J = 4.8 Hz), 7.58 (t, 1H, J = 4.8 Hz), 7.50 (dd, 1H, J = 2.8 Hz), 3.82 (dd, 2H, J = 4.8 Hz), 3.62 (dd, 2H, J = 5.2 Hz), 2.78 (m, 6H), 2.08 (s, 2H), 1.56 (m, 6H), 1.08 (d, 6H, J = 4.8 Hz).

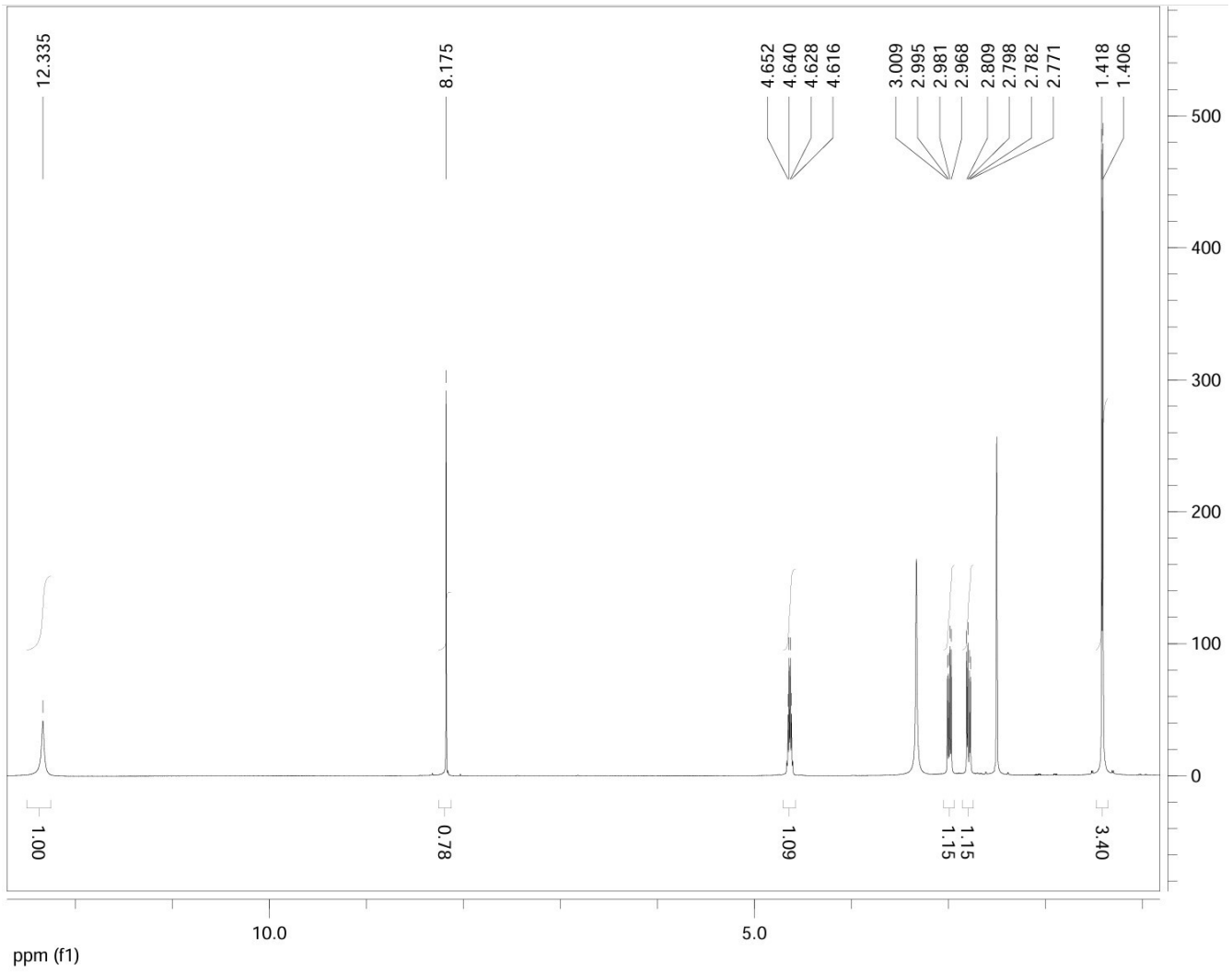

Figure S1. ^{1}H NMR spectrum of host **1** in DMSO-d_6 (400 MHz FT-NMR instrument).

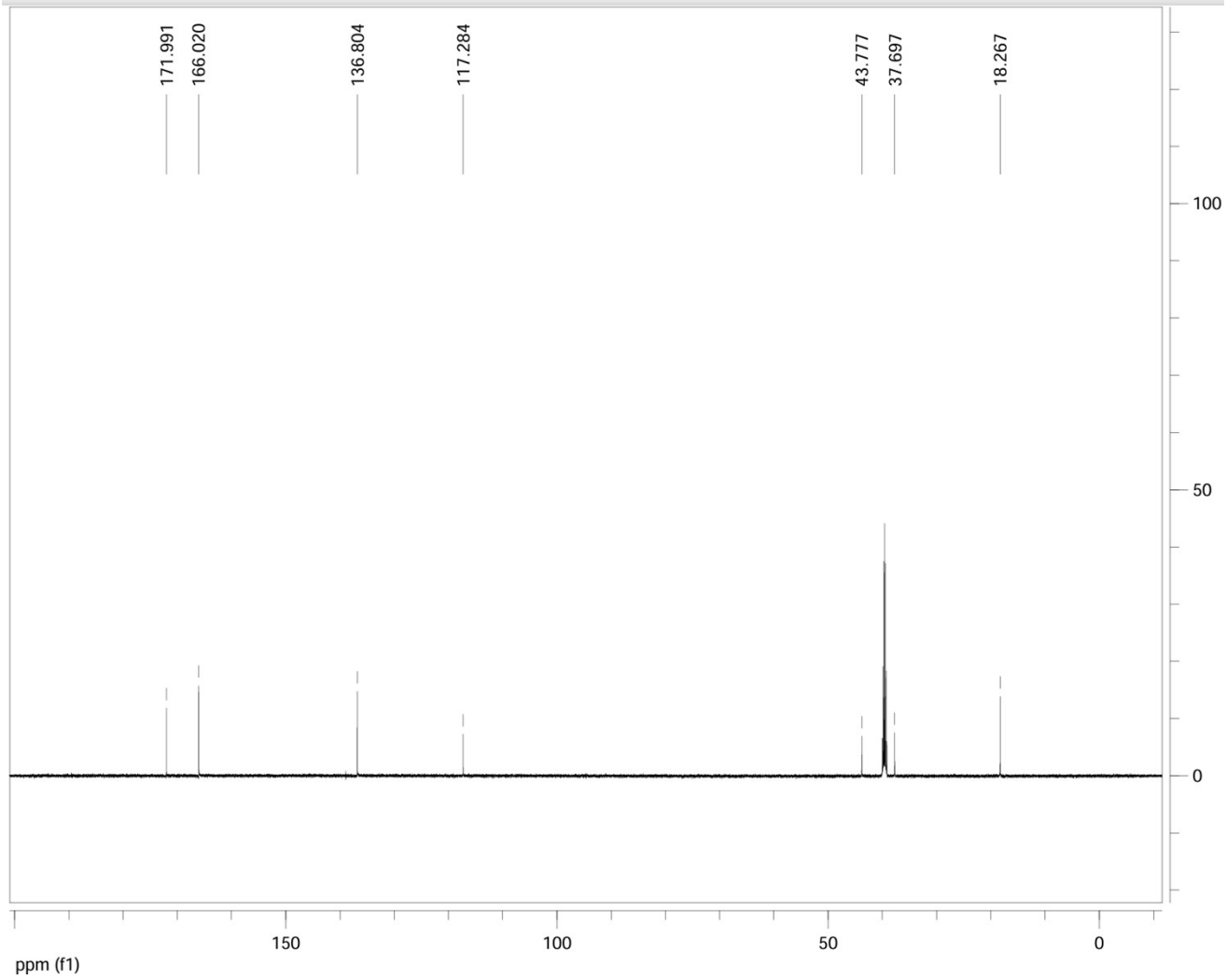

Figure S2. ^{13}C NMR spectrum of host **1** in DMSO-d_6 (400 MHz FT-NMR instrument).

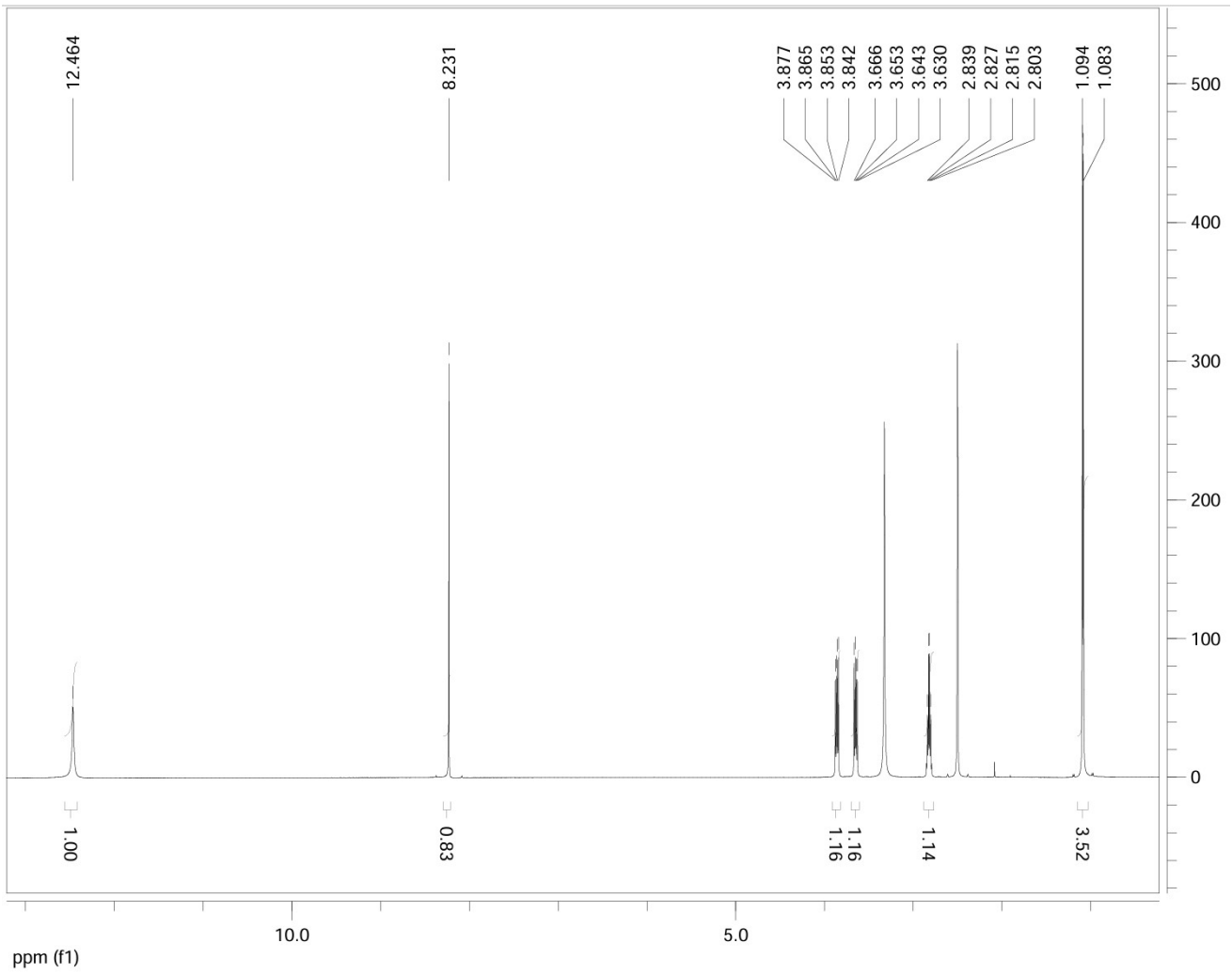

Figure S3. ^{1}H NMR spectra of host **2** in DMSO-d_6 (400 MHz FT-NMR instrument).

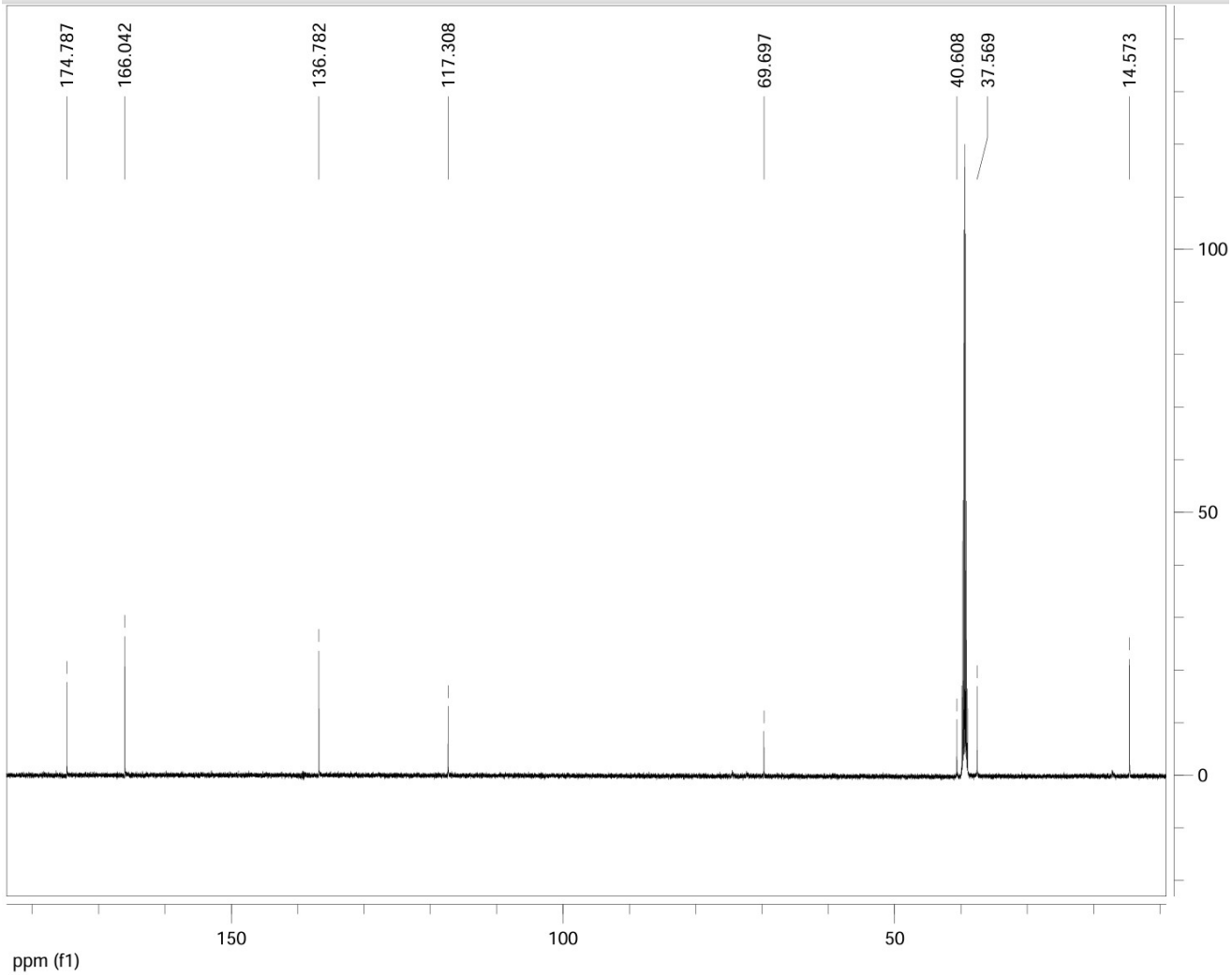

Figure S4. ^{13}C NMR spectra of host **2** in DMSO-d_6 (400 MHz FT-NMR instrument).

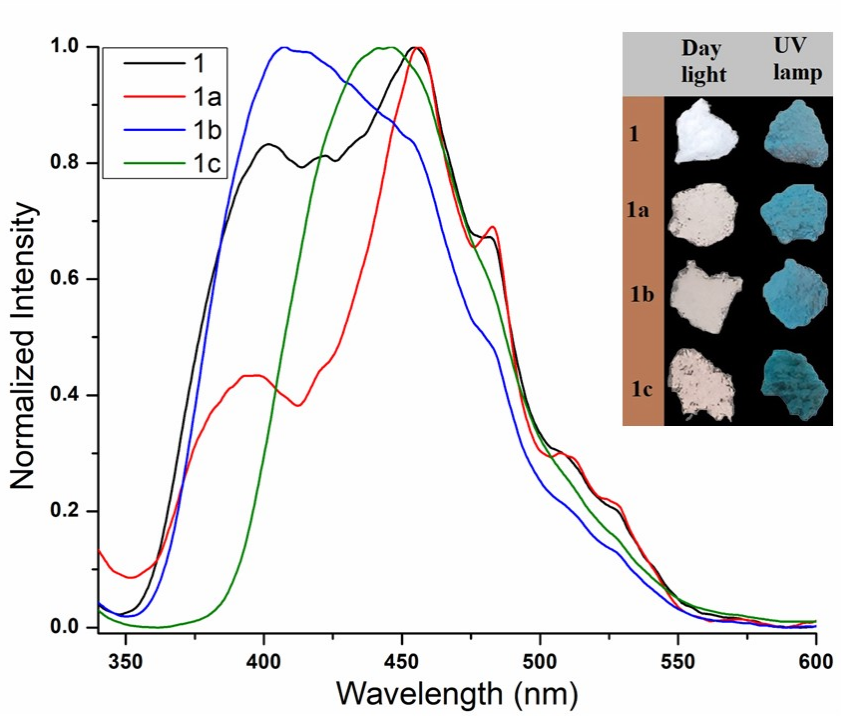

Figure S5. Normalised emission spectra along with the photographs of ground samples of host **1** and its solvates **1a**, **1b** and **1c**.

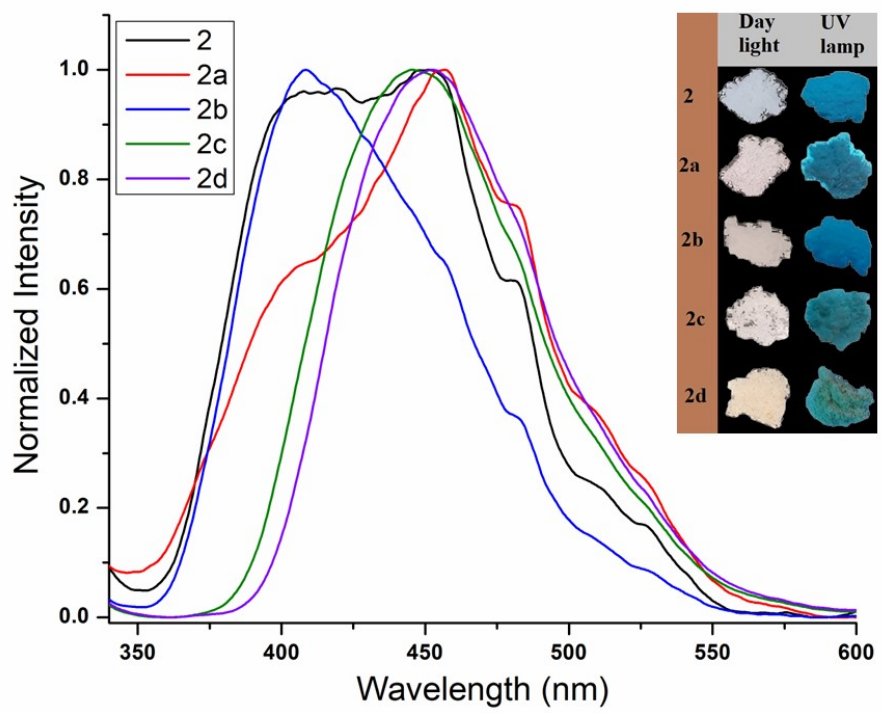

Figure S6. Normalised emission spectra along with the photographs of ground samples of host **2** and its solvates **2a**, **2b**, **2c** and **2d**.

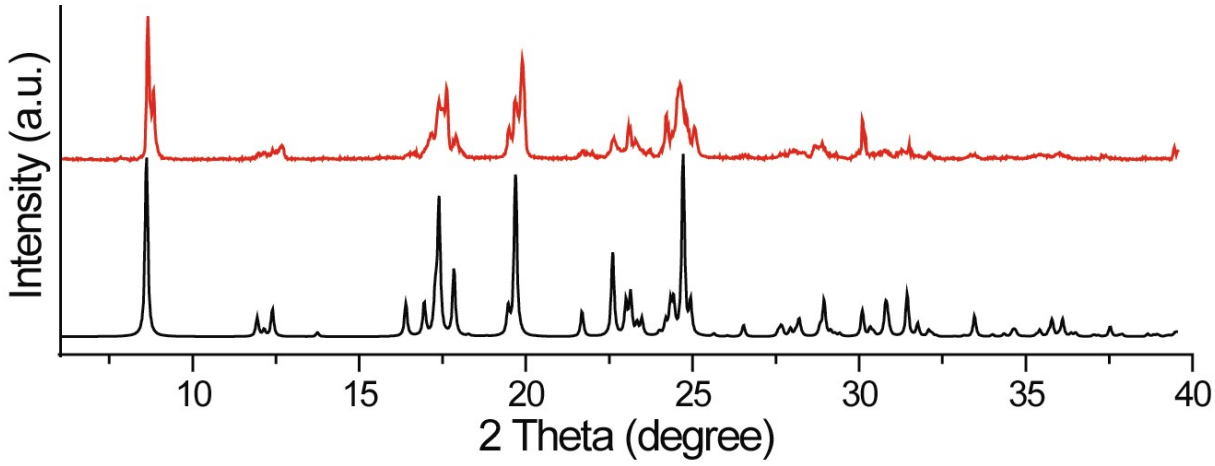

Figure S7. Simulated (black) and experimental (red) PXRD patterns of solvate **1a**.

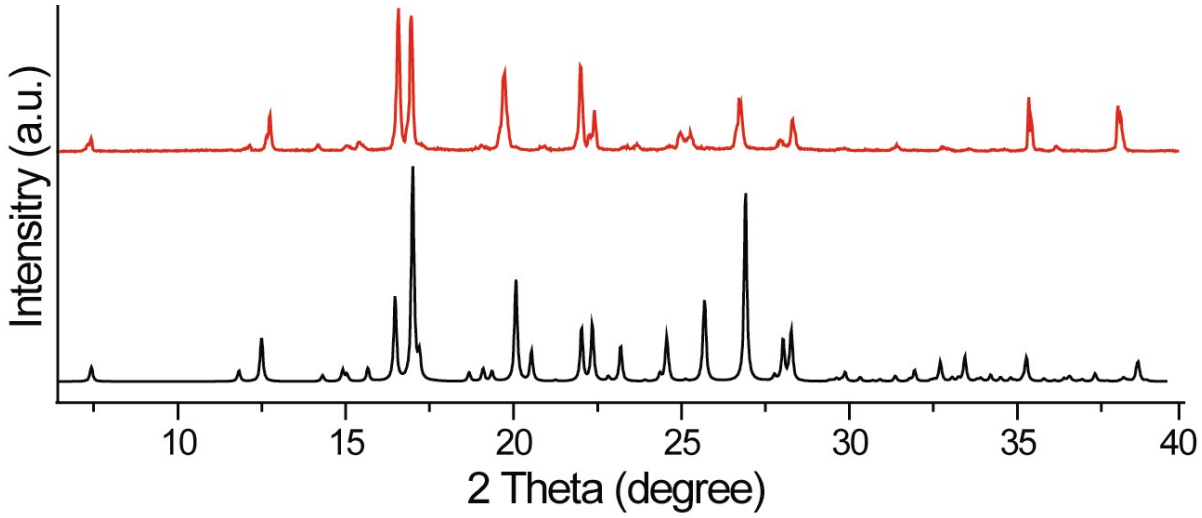

Figure S8. Simulated (black) and experimental (red) PXRD patterns of solvate **1b**.

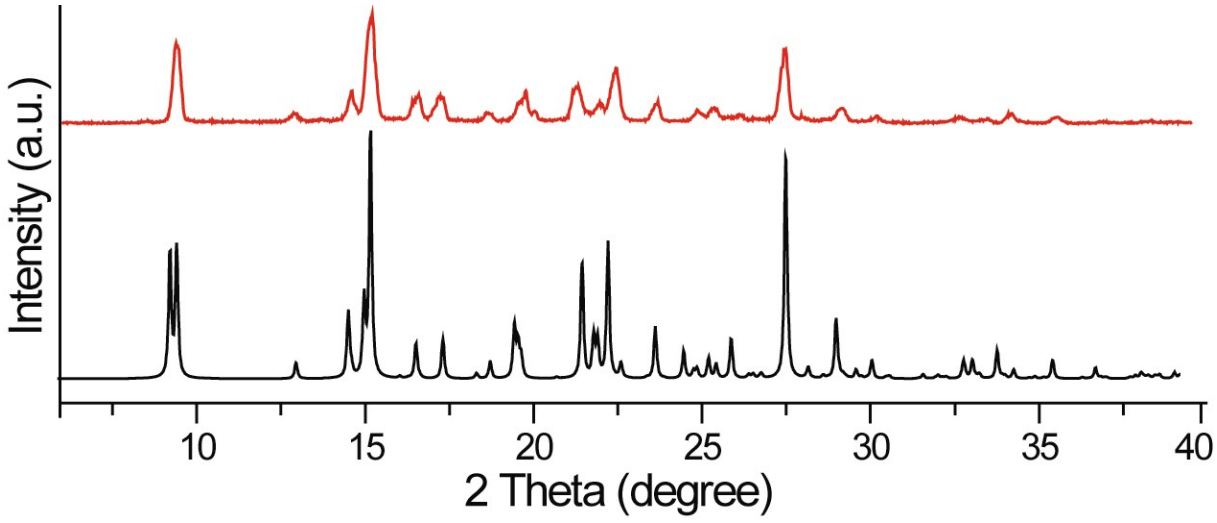

Figure S9. Simulated (black) and experimental (red) PXRD patterns of solvate **1c**.

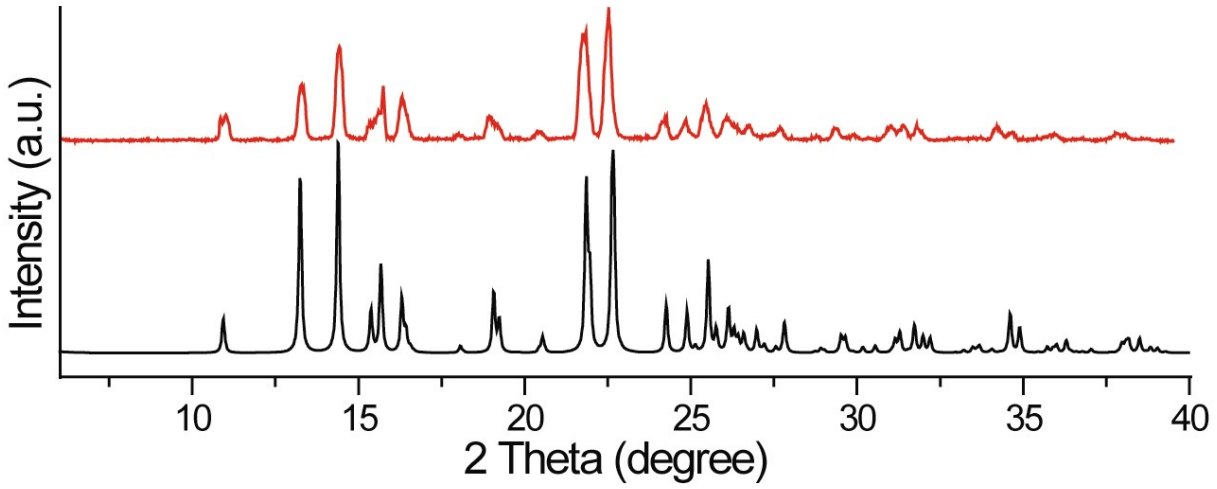

Figure S10. Simulated (black) and experimental (red) PXRD patterns of solvate **2a**.

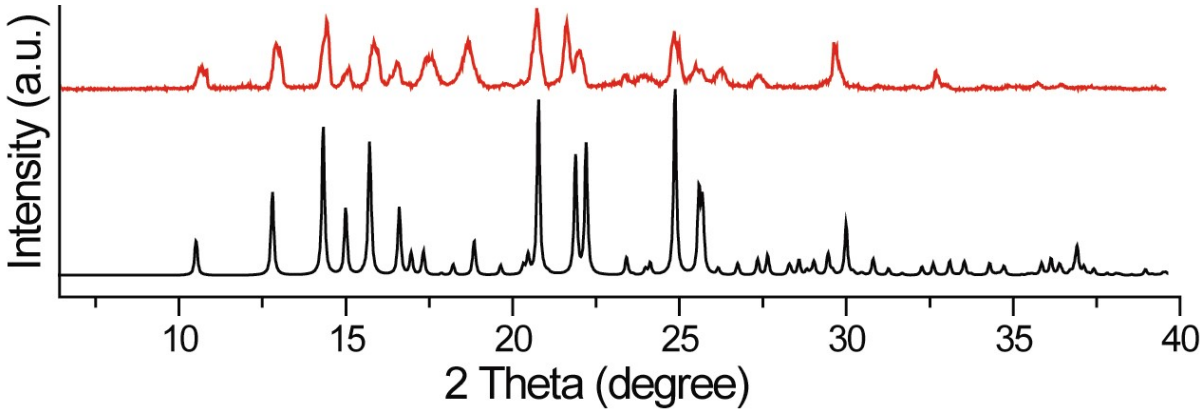

Figure S11. Simulated (black) and experimental (red) PXRD patterns of solvate **2b**.

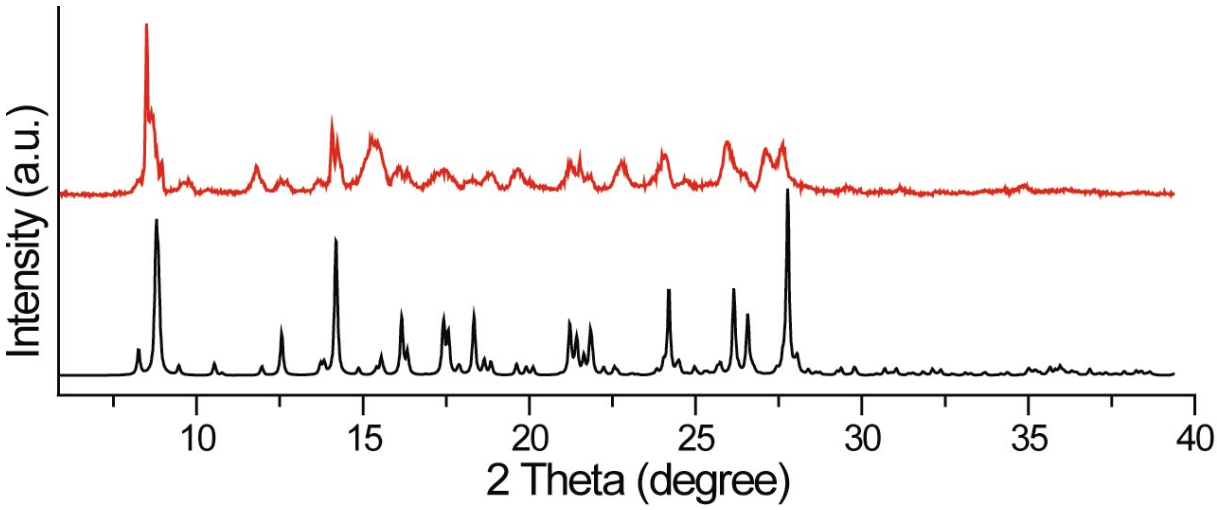

Figure S12. Simulated (black) and experimental (red) PXRD patterns of solvate **2c**.

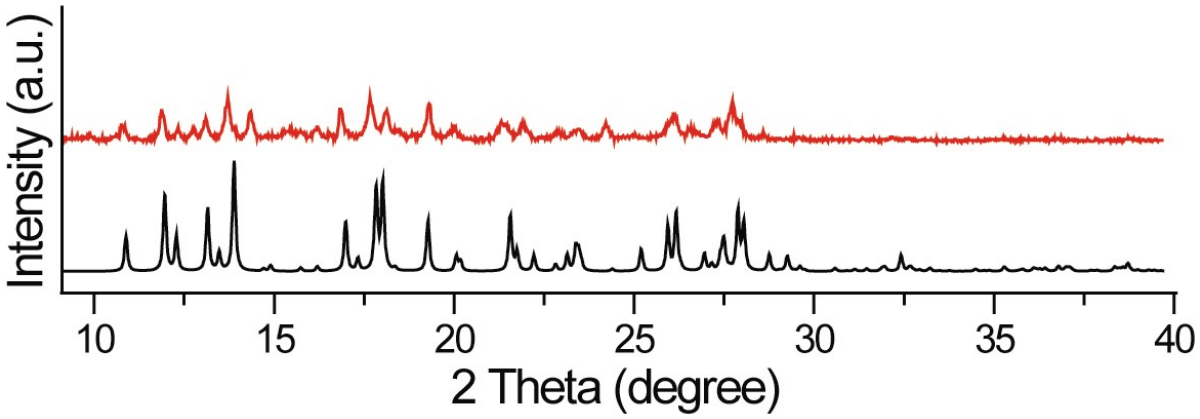

Figure S13. Simulated (black) and experimental (red) PXRD patterns of solvate **2d**.

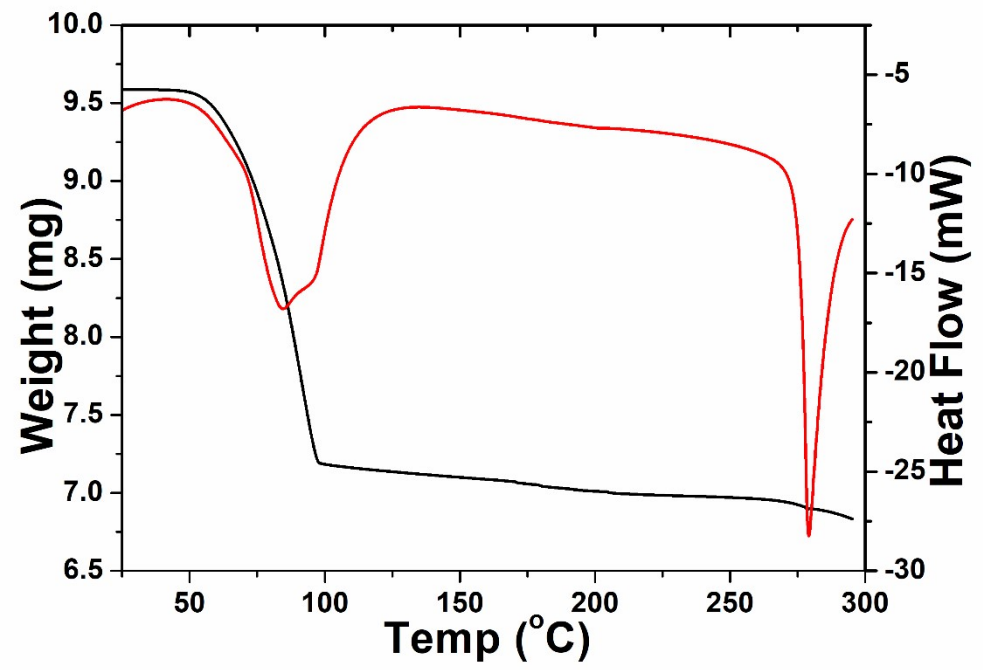

Figure S14. TGA (black) and DSC (red) curves of solvate **1a**.

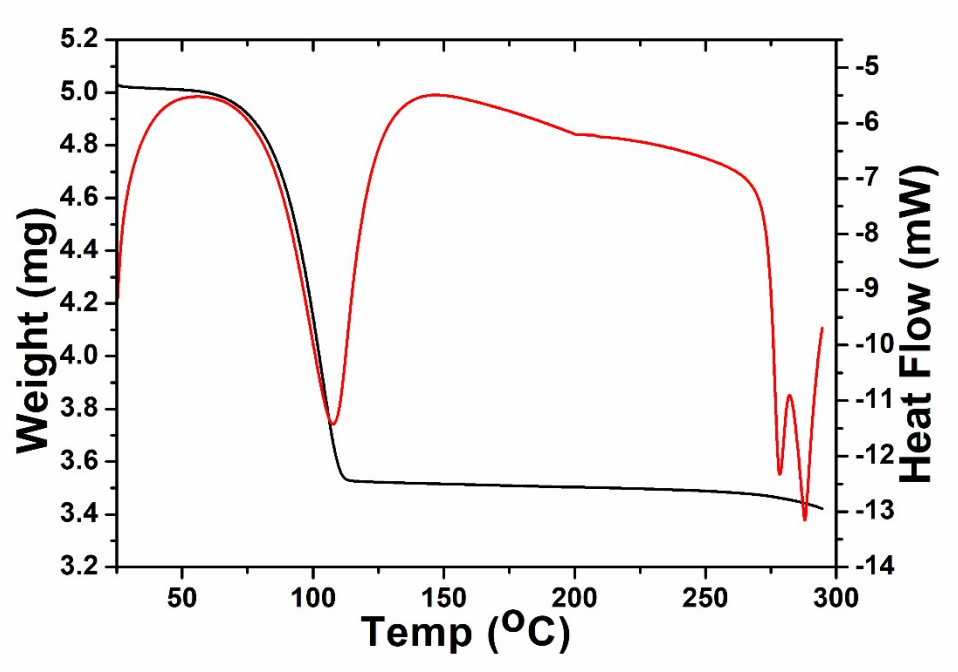

Figure S15. TGA (black) and DSC (red) curves of solvate **1b**.

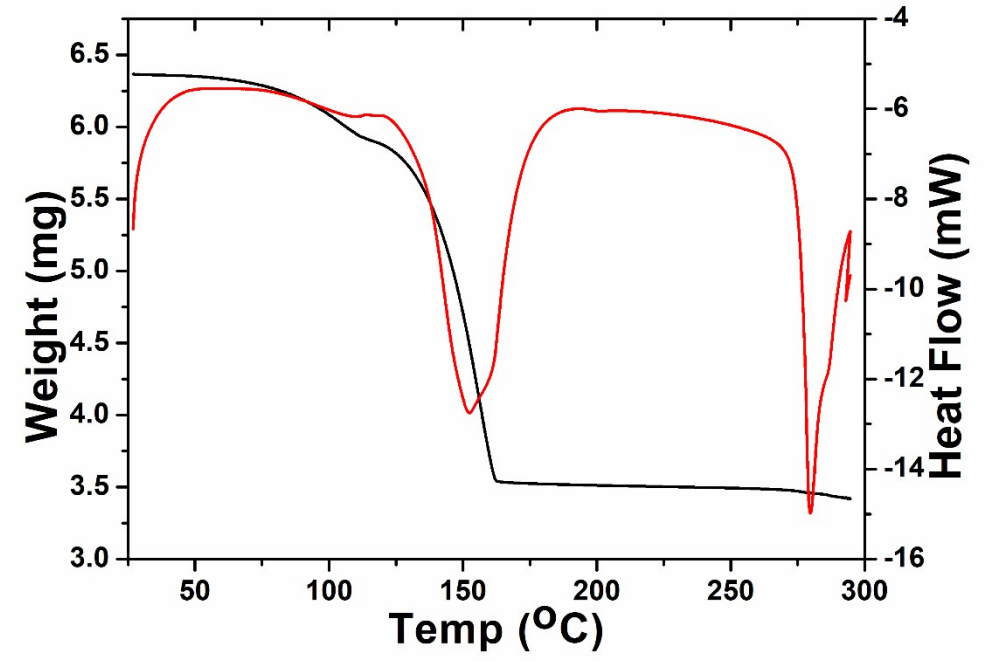

Figure S16. TGA (black) and DSC (red) curves of solvate **1c**.

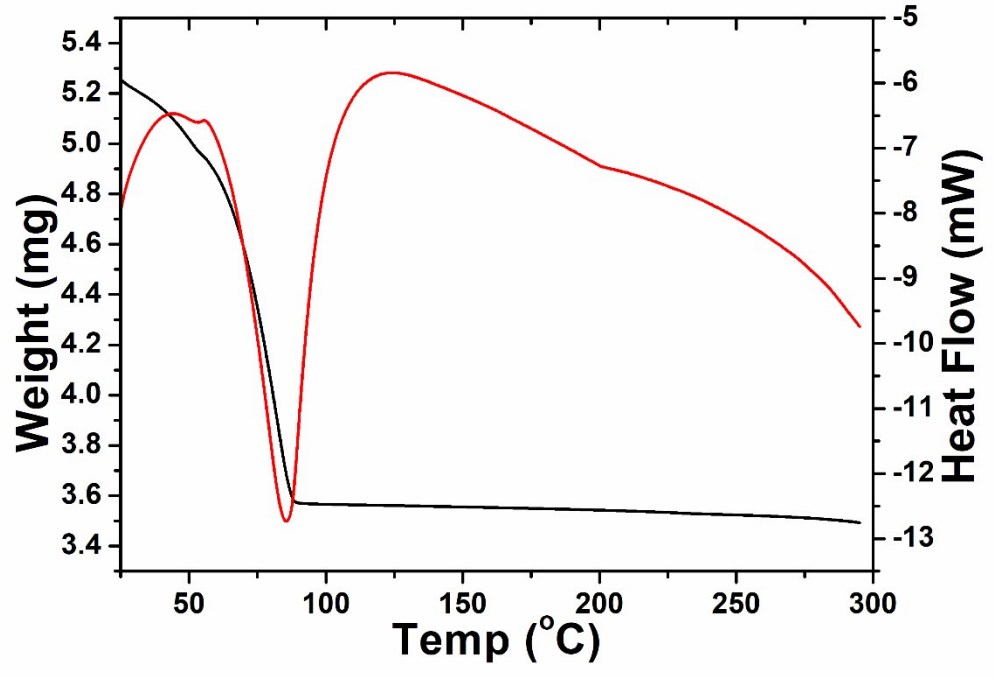

Figure S17. TGA (black) and DSC (red) curves of solvate **2a**.

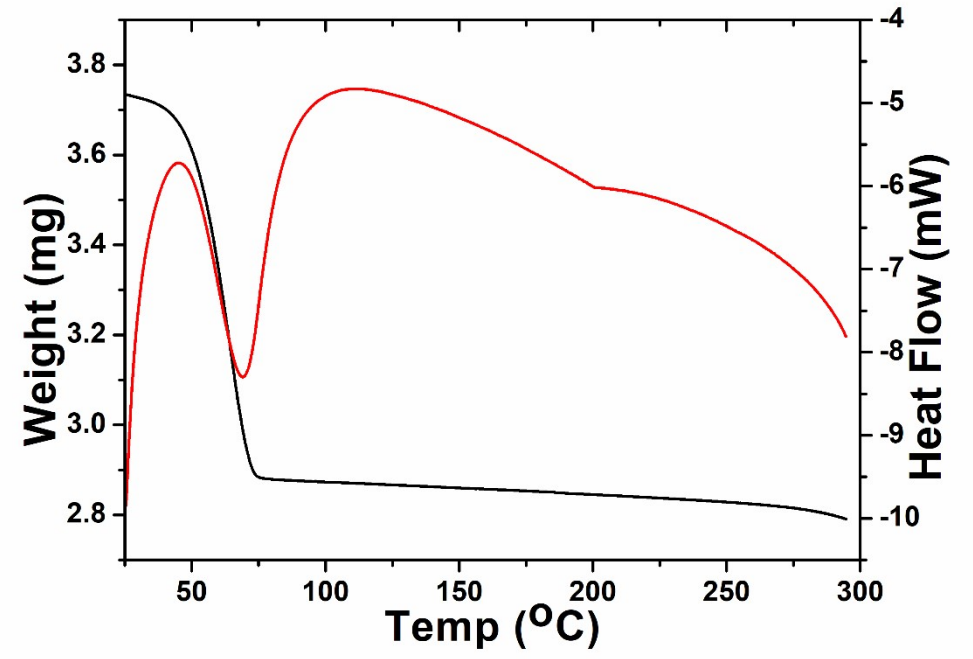

Figure S18. TGA (black) and DSC (red) curves of solvate **2b**.

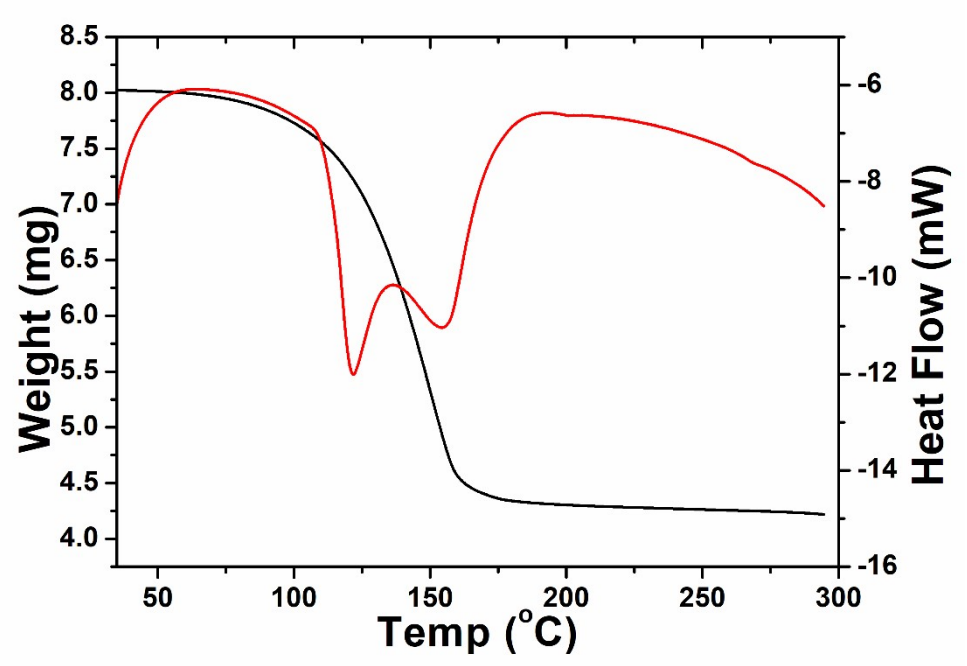

Figure S19. TGA (black) and DSC (red) curves of solvate **2c**.

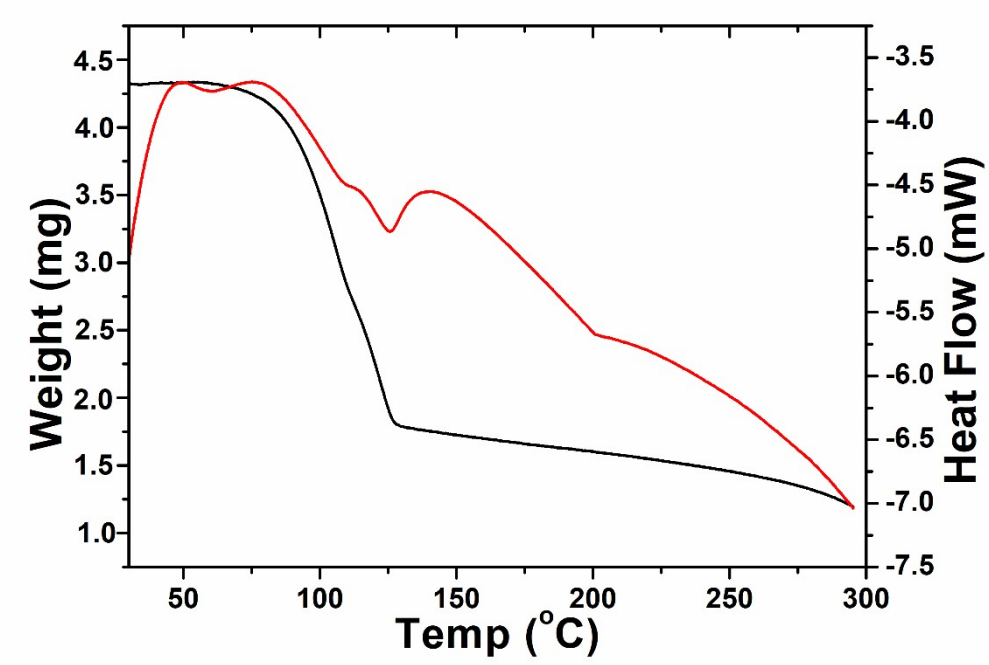

Figure S20. TGA (black) and DSC (red) curves of solvate **2d**.

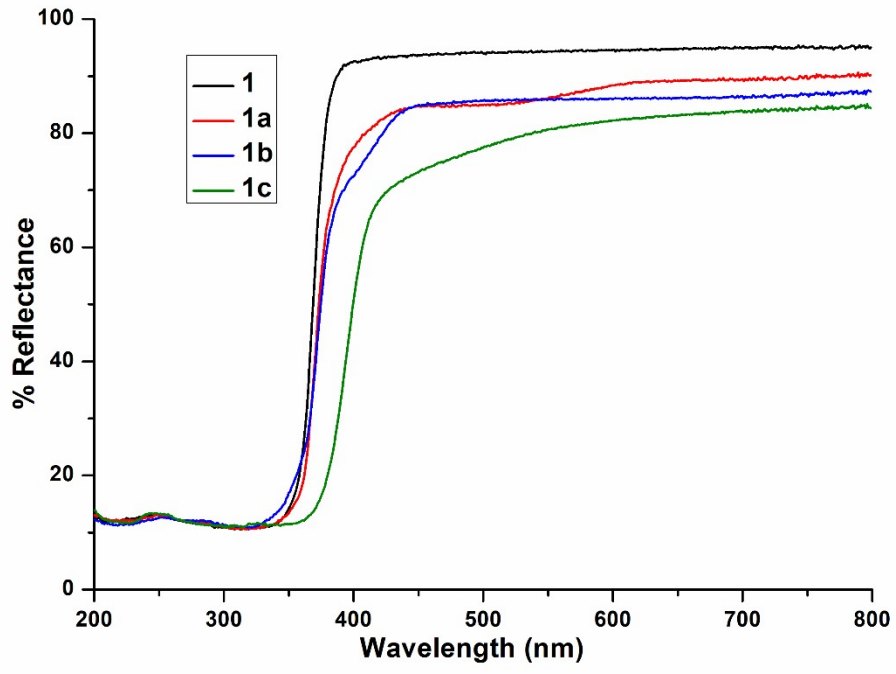

Figure S21. UV-Vis diffuse reflectance spectra of host **1** and its solvates **1a**, **1b** and **1c**.

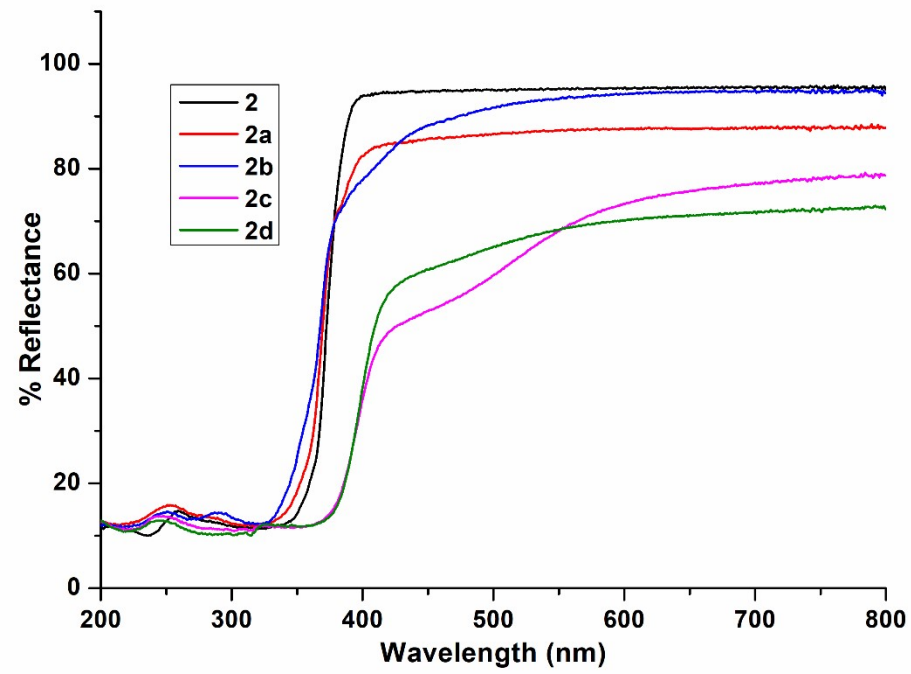

Figure S22. UV-Vis diffuse reflectance spectra of host **2** and its solvates **2a**, **2b**, **2c** and **2d**.

Table S1 Calculated interaction energies (E_{int}) at different basis sets and differences in E_{int} of the optimized structures (in eV).

Functional/Basis sets	Interaction energies (E_{int})		Relative stabilities
	3a	**3c**	Stability of **3a** over **3c**
B3LYP/6-31+G*	-7.4430	-6.5270	0.9160
B3LYP/6-31++G*	-7.0742	-6.5626	0.5116
B3LYP/6-31+G**	-8.5083	-7.9430	0.5653
AUG-cc-pVDZ	-10.1790	-9.6022	0.5768
	3b	**3d**	Stability of **3d** over **3b**
B3LYP/6-31+G*	-11.4450	-11.5357	0.0907
B3LYP/6-31++G*	-11.0634	-12.6610	1.5976
B3LYP/6-31+G**	-12.2870	-12.9110	0.6240
AUG-cc-pVDZ	-13.8498	-14.4675	0.6177

Table S2 Calculated interaction energies (E_{int}) at different basis sets and differences in E_{int} of the optimized structures (in eV).

Functional/Basis sets	Interaction energies (E_{int})		Relative stabilities
	6a	**6c**	Stability of **6a** over **6c**
B3LYP/6-31+G*	-12.4450	-4.0820	-8.3630
B3LYP/6-31++G*	-12.4640	-4.0093	-8.3647
B3LYP/6-31+G**	-13.2640	5.0489	-8.2151
AUG-cc-pVDZ	-13.6825	-6.4721	-7.2104
	6b	**6d**	Stability of **6b** over **6d**
B3LYP/6-31+G*	-12.4942	-6.9809	-5.8133
B3LYP/6-31++G*	-12.9875	-7.2104	-5.7771
B3LYP/6-31+G**	-13.2695	-7.9170	-5.5250
AUG-cc-pVDZ	-13.6892	-9.3483	-4.3409

Table S3. Calculated interaction energies (E_{int}) at different basis sets of B3LYP-D3 functional and differences in E_{int} of the optimized structures (in eV).

Functional/Basis sets	E_{int} (eV)	E_{int} (eV)	ΔE_{int} (eV)
	3a	**3b**	
B3LYP-D3/6-31+G*	-7.8497	-11.9917	4.1420
B3LYP-D3/6-31++G*	-7.8797	-11.8809	4.0012
B3LYP-D3/6-31+G**	-9.1164	-12.9927	3.8763
	3c	**3d**	
B3LYP-D3/6-31+G*	-7.2266	-12.4158	5.1892
B3LYP-D3/6-31++G*	-6.8253	-12.9457	6.1204
B3LYP-D3/6-31+G**	-8.6443	-13.6594	5.0151
	6a	**6b**	
B3LYP-D3/6-31+G*	-12.9547	-12.9442	-0.0105
B3LYP-D3/6-31++G*	-13.2140	-13.5427	0.3287
B3LYP-D3/6-31+G**	-13. 9754	-13.8745	-0.1009
	6c	**6d**	
B3LYP-D3/6-31+G*	-5.2502	-7.2141	1.9639
B3LYP-D3/6-31++G*	-5.5471	-7.6425	2.0954
B3LYP-D3/6-31+G**	-5.9871	-8.3124	2.3253

Table S4. Crystallographic parameters of solvates **1a**, **1b** and **1c**.

Compounds	**1a**	**1b**	**1c**
Empirical formula	$C_{24}H_{30}N_4O_{10}$	$C_{28}H_{26}N_4O_8$	$C_{36}H_{30}N_4O_8$
Formula weight	534.52	556.54	646.64
Wavelength	0.71073 Å	0.71073 Å	0.71073 Å
Crystal system	Monoclinic	Triclinic	Triclinic
Space group	$P2_1/n$	P-1	P-1
Unit cell dimensions (Å)	a = 11.884(2) b = 9.934(2) c = 12.344(3)	a = 6.6234(13) b = 7.8504(16) c = 12.820(3)	a = 6.8709(14) b = 10.625(2) c = 11.972(2)
Volume ($Å^3$)	1312.1(6)	646.9(2)	773.4(3)
Z	2	1	1
Density (Mg/m^3)	1.353	1.403	1.388
Abs coeff (mm^{-1})	0.106	0.105	0.100
F(000)	564	286	338
Index ranges	−15<=h<=15, −12<=k<=12, −15<=l<=14	−8<=h<=8, −10<=k<=10, −15<=l<=16	−8<=h<=8, −12<=k<=12, −14<=l<=14
Completeness to 2θ	99.8 %	99.1 %	99.8 %
Data / restraints / parameters	2976 / 0 / 176	2938 / 0 / 183	2716 / 0 / 218
Gof (F^2)	1.042	0.9930	1.021
R indices [I>2σ(I)]	R1 = 0.0704, wR2 = 0.1785	R1 = 0.0467, wR2 = 0.1003	R1 = 0.0896, wR2 = 0.1928
R indices (all data)	R1 = 0.0965, wR2 = 0.1925	R1 = 0.0886, wR2 = 0.1245	R1 = 0.2190, wR2 = 0.2614
CCDC No.	2324804	2324805	2324809

Table S5. Crystallographic parameters of solvates **2a**, **2b**, **2c** and **2d**.

Compounds	**2a**	**2b**	**2c**	**2d**
Empirical formula	$C_{24}H_{30}N_4O_{10}$	$C_{28}H_{26}N_4O_8$	$C_{36}H_{30}N_4O_8$	$C_{37}H_{45}N_5O_8$
Formula weight	534.52	546.53	646.64	687.78
Wavelength	0.71073 Å	0.71073 Å	0.71073 Å	0.71073 Å
Crystal system	Monoclinic	Monoclinic	Triclinic	Triclinic
Space group	$P2_1/c$	$P2_1/c$	P-1	P-1
Unit cell dimensions (Å)	a = 16.173(3) b = 7.3318(19) c = 11.298(2)	a = 16.796(3) b = 7.5311(15) c = 10.637(2)	a = 10.925(2) b = 12.294(3) c = 13.214(3)	a = 6.8672(14) b = 7.5914(15) c = 16.850(3)
Volume ($Å^3$)	1339.6(5)	1340.0(5)	1553.6(5)	857.2(3)
Z	2	2	2	1
Density (Mg/m^3)	1.325	1.355	1.382	1.332
Abs coeff (mm^{-1})	0.104	0.101	0.099	0.095
F(000)	564	572	676	366
Index ranges	–20<=h<=20, –8<=k<=9, –14<=l<=14	–21<=h<=21, –9<=k<=9, –13<=l<=13	–14<=h<=14, –15<=k<=15, –16<=l<=17	–7<=h<=8, –8<=k<=8, –20<=l<=20
Completeness to 2θ	99.7 %	99.7 %	98.3 %	99.5 %
Data / restraints / parameters	3069 / 0 / 177	3061 / 0 / 212	6979 / 0 / 435	3001 / 7 / 267
Gof (F^2)	1.095	1.109	1.032	1.063
R indices [I>2σ(I)]	R1 = 0.0628, wR2 = 0.1556	R1 = 0.0796, wR2 = 0.1861	R1 = 0.1153, wR2 = 0.2974	R1 = 0.1057, wR2 = 0.2896
R indices (all data)	R1 = 0.1298, wR2 = 0.1999	R1 = 0.0953, wR2 = 0.1959	R1 = 0.2359, wR2 = 0.3779	R1 = 0.1748, wR2 = 0.3476
CCDC No.	2324806	2324807	2324808	2324810

Table S6. Hydrogen bond parameters (Å and °) of solvates **1a**, **1b**, **1c** and **2a, 2b, 2c**, **2d**.

Compounds	D-H···A	d_{D-H}	$d_{H...A}$	$d_{D...A}$	∠D-H···A
1a	O3-H3···O1D [-x+2, -y, -z+1]	0.84	1.76	2.6(16)	170
	C1D-H1D···O1 [2-x, -y, 1-z]	0.95	2.45	3.36	173.9
	C2D-H2D3···O4 [1+x, y, z]	0.98	2.59	3.53	168.3
	C8-H8B···O3 [x, -1+y, z]	0.98	2.82	3.64	170
1b	O3-H3···N1P [-x, -y, -z+2]	0.83	1.79	2.63(15)	173.6
	C1P-H1P···O3	0.97	2.82	3.47	156.6
	C2P-H2P···O2 [x, -1+y, z]	0.97	2.85	3.56	175.5
	C3P-H3P···O1 [-x, -½+y, ½-z]	0.97	2.48	3.41	136.5
	C4P-H4P···O4	0.97	2.68	3.61	121.6
	C5P-H5P···O4	0.97	2.70	3.64	124.7
1c	O3-H3···N1Q [-x, -y+1, -z+1]	0.84	1.82	2.65(2)	173.9
	C3Q-H3Q···O1 [-1+x, y, z]	0.98	2.52	3.30	122.1
	C6Q-H6Q···O2 [1+x, 1+y, -1+z]	0.98	2.78	3.58	162.9
2a	O3-H3···O1D [-x+1, -y+2, -z+1]	0.84	1.74	2.58(14)	170.9
	C1D-H1D···O4	0.95	2.48	3.20	124.5
	C3D-H3D3···O3	0.98	2.98	3.64	161.9
	C2D-H2D1···O2 [x, 1+y, z]	0.98	2.87	3.60	159.2
	C3-H3···O1 [1-x, 2-y, 1-z]	0.98	2.45	3.27	128.5
	C9-H9A···O2	0.98	2.77	3.57	166.4
2b	O3-H3···N1P [-x+1, -y+1, -z]	0.84	1.90	2.75(19)	177.1
	C1P-H1P···O4 [x, -1+y, z]	0.98	2.31	3.12	129.3
	C2P-H2P···O4	0.98	2.78	3.46	138.6
	C3P-H3P···O4	0.98	2.85	3.56	151.7
	C5P-H5P···O1 [x, ½-y, -½+z]	0.99	2.38	3.22	150.9
	C81-H81···O1 [-x, -½+y, ½-z]	0.98	2.92	3.67	168.7
	C3-H3A···O2	0.98	2.50	3.26	137.5
2c	O7-H7···N1Q [-x+1, -y, -z+1]	0.84	1.83	2.67 (3)	154.4
	O5-H5···N2Q [x, 1-y, 1-z]	0.84	1.88	2.62	144.3
	C7Q-H7Q···O4 [-x, 1-y, 1-z]	0.99	2.32	3.29	144.3
	C10Q-H10Q···O8 [-x, 1-y, 1-z]	0.99	2.80	3.47	145.6
	C12Q-H12Q···O8	0.98	2.47	3.25	160.0

2d	C15Q-H15Q···O1 [-x, -½+y, ½-z]	0.99	2.56	3.37	156.4
	C3-H3···O6	0.99	2.47	3.46	157.2
	C2P-H2P1-O41 [x, 1-y, 1-z]	0.99	1.90	2.67	157.3
	C2P-H2P2···O31 [-x, 1-y, 1-z]	0.99	1.95	2.72	169.5
	C4P-H4P1···O1 [-x, 1-y, 1-z]	0.99	2.65	3.61	159
	C1P-H1P1···O1	0.99	2.60	3.59	170.8
	C3-H3···O2	0.98	2.86	3.28	127

References

S1. *GAUSSIAN03, Revision B.05*; Gaussian, Inc.: Pittsburgh, PA, 2003.

S2. P. Hohenberg and W. Kohn, *Phys. Rev.*, 1964, **136**, B864–B871.

S3. A. D. Becke, *J. Chem. Phys.*, 1993, **98**, 5648–5652.

S4. C. Lee, W. Yang and R. G. Parr, *Phys. Rev. B: Condens. Matter Mater. Phys.*, 1988, **37**, 785–789.

S5. Rapid Auto software, R-Axis series, Cat. No. 9220B101, Rigaku Corporation.

S6. G. M. Sheldrick, *ActaCrystallogr. A: Found. Adv.*, 2008, **A64**, 112–122.